Global Compartmental Analysis of the Fluorescence Decay Surface of the Halato Telechelic Polymer (*N*,*N*-Dimethyl-*N*-[3-(1-pyrenyl)propyl]ammonio)-trifluoromethanesulfonate-End-Capped Poly(tetrahydrofuran)

Bart Hermans,[†] Frans C. De Schryver,*[,†] Jan van Stam,[†] Noël Boens,[†] Robert Jérôme,[‡] Philippe Teyssié,[‡] Geert Trossaert,[§] Erik Goethals,[§] and Etienne Schacht[§]

Department of Chemistry, Katholieke Universiteit Leuven, B-3001 Heverlee, Belgium, Université de Liège, Sart-Tilman, B-4000 Liège, Belgium, and Rijksuniversiteit Gent, B-9000 Gent, Belgium

Received November 28, 1994; Revised Manuscript Received February 15, 1995[⊗]

ABSTRACT: The kinetic behavior of the halato telechelic polymer (*N*,*N*-dimethyl-*N*-[3-(1-pyrenyl)propyl]-ammonio)trifluoromethanesulfonate-end-capped poly(tetrahydrofuran) (POLYPROBE) in tetrahydrofuran is investigated by global compartmental analysis of the fluorescence decay surface. At low POLYPROBE concentrations the emission decays monoexponentially. When an analogous end-capped halato telechelic polymer without the pyrene chromophore ((*N*,*N*,*N*-triethylammonio)trifluoromethanesulfonate-end-capped poly(tetrahydrofuran), POLYSALT) is added to solutions containing a low POLYPROBE concentration, the emission can be fitted by a biexponential decay function. From these observations it is concluded that the second excited-state species in the POLYPROBE−POLYSALT system is POLYPROBE involved in ion aggregation due to dipole−dipole or ion−dipole interaction. At higher POLYPROBE concentrations, without added POLYSALT, a triexponential decay function is needed to describe the emission. The third excited-state species is a POLYPROBE excimer, which can be formed via two pathways: either intermolecularly when a locally excited POLYPROBE encounters a ground-state POLYPROBE or intramolecularly when an aggregate of two POLYPROBE molecules rearranges. From the global compartmental analysis in which the value of one of the rate constants is scanned, it is found that the bimolecular processes are slowed down by the presence of the polymer chain, while intramolecular rearrangements are not affected.

1. Introduction

The introduction of ionic units on neutral polymers drastically changes the properties of these materials, which can be readily found by various methods, e.g., viscosity and scattering measurements.[1−6] It is clear that the behavior of these charged materials will depend strongly on the dielectric constant of the solvent. In polar solvents the counterions will be readily solvated, resulting in a polymer backbone that covalently links several free charges. The electrostatic forces are important, and the way these polyelectrolytes behave in polar solvents is known in the literature as the polyelectrolyte behavior. In less polar solvents ($\epsilon < 15$) the counterions will stay closer to the ionic units on the chain. Due to the ion−ion interactions, contact ion pairs and/or solvent-separated ion pairs are more likely to be formed than free ions. These contact ion pairs can be regarded as dipoles, and ion−dipole and dipole−dipole interactions occur in these media.[7] In the literature the former is referred to as the ion aggregate behavior.

Initially[1−6] ionomers based on sulfonate and carboxylate groups were studied by viscometry. The characteristic behavior of the reduced viscosity with the concentration in apolar solvents, which differs from the linear behavior of neutral polymers, can generally be described in the follow way. At low ionomer concentrations the reduced viscosity is less than that of the corresponding polymer. In this region intrachain interactions are thought to be dominant. Increasing the concentration increases the reduced viscosity more steeply than the linear increase of the neutral polymer system. This is interpreted as a growing importance and finally the predominance of the interchain associations. Additional information on the aggregation was obtained by light scattering measurements.[3,8,9] Further refinement of the model describing the aggregation phenomenon was obtained through neutron scattering.[10−12] Besides the dipole−dipole interaction, entropy changes emanating from the transition from an individual chain to an aggregate have to be taken into account. It is generally accepted that most systems can be described by the open association model in which an equilibrium is formed between single chains and aggregates of all sizes. Small-angle X-ray scattering and transmission electron microscopy were used to prove the occurrence of chain extension.[13] The microdomains formed by ionomers in nonpolar solvents were investigated in detail using fluorescent probes.[14,15]

Further investigation of chain and medium characteristics resulted in modeling the ionomers by halato telechelic polymers. These are polymers with one or more ends capped with ionic units. Depending on the solvent, even halato telechelic polymers exhibit one of the two behaviors described above. The ion aggregation of this class of polymers in apolar solvents was closely examined by viscosity measurements.[16−21] Although these chains only bear two ionic units, the same model based on ion pair aggregation is thought to be valid.[8]

Since the intra- and interchain interactions play an important role, intra- and intermolecular excimer formation was used to obtain more information about the association.[22] For that purpose a fluorescent probe was

* To whom correspondence should be addressed.
† Katholieke Universiteit Leuven.
‡ Université de Liège.
§ Rijksuniversiteit Gent.
⊗ Abstract published in *Advance ACS Abstracts,* April 1, 1995.

0024-9297/95/2228-3380$09.00/0

attached to both ends of a polystyrene halato telechelic polymer. Stationary fluorescence measurements were an excellent method to discriminate between intra- and interchain associations. The scheme presented also indicates a concentration region where the intrachain dipole–dipole interactions prevail, and a transition to dominance of interchain interactions occurs on increasing the concentration.

It should be noted that all schemes presented and all data confirming these models describe a static view of the ion aggregation behavior. By time-resolved fluorescence spectroscopy it should be possible to obtain more detailed kinetic information about this phenomenon. Halato telechelic polymers that carry chromophores at one or more ends can be used for this purpose. To understand the information obtained by a chromophore-capped polymer backbone, however, the kinetic behavior of the probe itself must first be elucidated. The kinetics of the charged fluorescent probe *N,N,N*-trimethyl-3-(1-pyrenyl)-1-propanaminium perchlorate were unraveled and were reported in a previous publication.[23] It was possible to determine all the rate constants within certain limits based on a kinetic scheme in which dipole–dipole association and excimer formation are taken into account. In this paper, we extend the study to a halato telechelic polymer. The fluorescent probe previously used[23] was attached to a poly(tetrahydrofuran). The aggregation phenomenon is studied in detail by time-resolved fluorescence measurements, and the fluorescence decay surface is evaluated by global compartmental analysis. From the results of the analysis a kinetic scheme will be proposed from which the ion aggregation behavior will be discussed.

2. Experimental Section

2.1. Materials. 1-pyrenecarbaldehyde, (carbethoxymethylene)triphenylphosphorane, toluene (99%), Pd/Cl, $LiAlH_4$, PBr_3, dichloromethane (>99%), triethylamine (>99%), and *tert*-butyl methyl ether were purchased from Janssen. Ethanol (>99%) was obtained from Merck, tetrahydrofuran (THF, HPLC) was supplied by Rathburn, and dimethylamine was supplied by UCAR.

2.2. Synthesis and Characteristics of (*N,N*-Dimethyl-*N*-[3-(1-pyrenyl)propyl]ammonio)trifluoromethanesulfonate-End-Capped Poly(tetrahydrofuran) (POLYPROBE) and (*N,N,N*-Triethylammonio)trifluoromethanesulfonate-End-Capped Poly(tetrahydrofuran) (POLYSALT). *N,N*-Dimethyl-3-(1-pyrenyl)-1-propanamine (PROBE) was synthesized as described previously.[23] Poly(tetrahydrofuran) was synthesized via cationic ring-opening polymerization with methyl triflate ($CF_3SO_3CH_3$) as initiator. The final products were obtained by termination of the polymerization by adding PROBE to obtain POLYPROBE or triethylamine to obtain POLYSALT.

The characteristics for the obtained products are as follows: POLYPROBE, M_n(GPC) = 4310, M_w(GPC) = 4790, M_w(NMR) = 4550; POLYSALT, M_n(GPC) = 4070, M_w(GPC) = 4670, M_w(NMR) = 4570. The structure of POLYPROBE is shown in Figure 1.

All solutions for fluorescence measurements were prepared in THF and degassed using five freeze–pump–thaw cycles prior to the measurements.

2.3. Absorption and Stationary and Time-Resolved Fluorescence Measurements. Absorption spectra were recorded on a Perkin-Elmer Lambda 6 UV/vis spectrophotometer coupled to a personal computer. Excitation spectra (emission wavelength: 378 nm) and the corrected steady-state fluorescence spectra (excitation wavelength: 344 nm) were recorded on an SLM Aminco 8000C spectrofluorimeter.

Fluorescence decay curves were obtained using a Spectra-Physics mode-locked, synchronously pumped, cavity-dumped, frequency-doubled DCM dye laser as the excitation source (excitation wavelength: 320 nm) with single-photon-timing

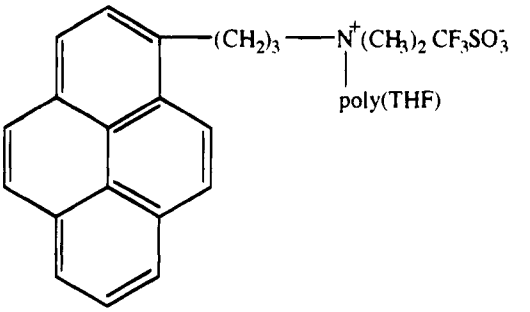

Figure 1. Structure of (*N,N*-dimethyl-*N*-[3-(1-pyrenyl)propyl]-ammonio)trifluoromethanesulfonate-end-capped poly(tetrahydrofuran) (POLYPROBE).

Scheme 1

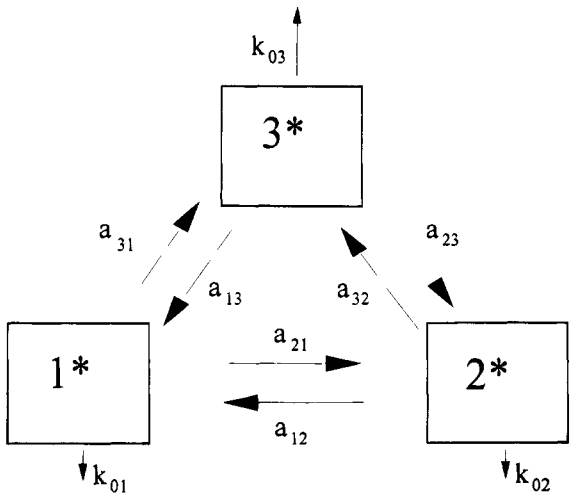

detection. A detailed description of the apparatus has been given elsewhere.[24] All decays had 512 data points with approximately 3000 counts in the peak channel. All solutions where excimers are formed were measured in the front-phase configuration using quartz cells with 1 mm path length. Low-concentration solutions were measured in the right angle configuration using quartz cells with 1 cm path length. The emission polarizer was set at the magic angle configuration. All measurements were performed at ambient temperature.

The fluorescence quantum yields of the probes were determined with quinine sulfate in 0.1 N sulfuric acid as a reference.[25] Correction for the refractive index was applied.

3. Theory and Data Analysis

3.1. Kinetics. Consider a causal, linear, time-invariant, photophysical system consisting of three distinct ground-state species (1, 2, 3) and three corresponding excited-state species (1*, 2*, 3*) as depicted in Scheme 1. The excited-state species can decay by fluorescence (F) and nonradiative processes (NR) (internal conversion (IC) and intersystem crossing (ISC)). The composite rate constants for these processes for species i^* are denoted by k_{0i} ($=k_{Fi} + k_{ICi} + k_{ISCi}$). The interconversion $j^* \rightarrow i^*$ is described by a_{ij}. The transformation can be either monomolecular ($a_{ij} = k_{ij}$) or bimolecular ($a_{ij} = k_{ij}$[M]), where k_{ij} denotes the rate constant for the interconversion and [M] is the concentration.

The theory of global bicompartmental analysis in the absence of an added quencher is thoroughly described,[26–28] and as this theory can easily be expanded to tricompartmental systems,[23] only the fundamental aspects will be presented here.

After excitation which does not significantly alter the concentrations of the ground-state species, the fluores-

Scheme 2

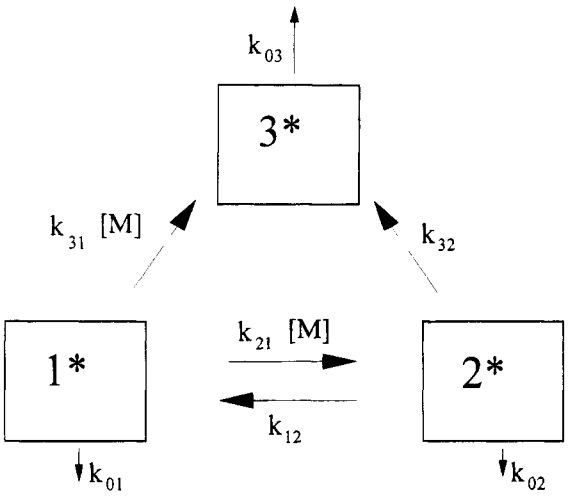

cence δ-response function, $f(\lambda^{em},\lambda^{ex},t)$, at emission wavelength λ^{em} due to excitation at λ^{ex} is expressed by[26]

$$f(\lambda^{em},\lambda^{ex},t) = \kappa\tilde{\mathbf{c}}(\lambda^{em})\mathbf{U}\exp(t)\mathbf{U}^{-1}\tilde{\mathbf{b}}(\lambda^{ex}) \qquad t \geq 0 \quad (1)$$

with κ a proportionality constant. $\mathbf{U} \equiv [\mathbf{U}_1,\mathbf{U}_2,\mathbf{U}_3]$ is the matrix of the three eigenvectors of matrix **A** (eq 2) and $\mathbf{U}^{-1}$ is the inverse of **U**. γ_1, γ_2, and γ_3 are the eigenvalues of **A** corresponding to $\mathbf{U}_1$, $\mathbf{U}_2$, and $\mathbf{U}_3$ and $\exp(t\gamma)$ diag$\{\exp(\gamma_1 t), \exp(\gamma_2 t), \exp(\gamma_3 t)\}$.

$$\mathbf{A} \equiv \begin{bmatrix} -(k_{01}+a_{21}+a_{31}) & a_{12} & a_{13} \\ a_{21} & -(k_{02}+a_{12}+a_{32}) & a_{23} \\ a_{31} & a_{32} & -(k_{03}+a_{13}+a_{23}) \end{bmatrix} \quad (2)$$

$\tilde{b}(\lambda^{ex})$ is the 3×1 matrix of the normalized absorbances $\tilde{b}$ of species i at λ^{ex}.

$$\tilde{b}_i = b_i/\sum b_i \qquad \text{for } i = 1, 2, 3 \quad (3)$$

$\tilde{c}(\lambda^{em})$ is the 1×3 matrix of the normalized spectral emission weighting factors $\tilde{c}$ of species i^* at λ^{em}.

$$\tilde{c}_i = c_i/\sum c_i \qquad \text{for } i = 1, 2, 3 \quad (4)$$

Equation 1 can be written in the triple-exponential format as

$$f(\lambda^{em},\lambda^{ex},t) = \sum_{i=1}^{3} \alpha_i \exp(\gamma_i t) \qquad t \geq 0 \quad (5)$$

Based on the analysis of the fluorescence decay data (vide infra) of POLYPROBE in tetrahydrofuran, a kinetic scheme can be proposed (Scheme 2). In this scheme the interconversions $1^* \rightarrow 2^* \rightarrow$ and $1^* \rightarrow 3^*$ are bimolecular and therefore are described by the second-order rate constants k_{21} and k_{31}, respectively. The processes $2^* \rightarrow 1^* \rightarrow$ and $2^* \rightarrow 3^*$ are monomolecular and are specified by the first-order rate constants k_{12} and k_{32}, respectively, and the interconversions $3^* \rightarrow 1^*$ and $3^* \rightarrow 2^*$ are negligibly slow. In this case matrix **A** (eq 2) can be simplified to

$$\mathbf{A} = \begin{bmatrix} -(k_{01}+k_{21}[\mathrm{M}]+k_{31}[\mathrm{M}]) & k_{12} & 0 \\ k_{21}[\mathrm{M}] & -(k_{02}+k_{12}+k_{32}) & 0 \\ k_{31}[\mathrm{M}] & k_{32} & -k_{03} \end{bmatrix} \quad (6)$$

The exponential factors γ_i are related to the decay times

$$\gamma_i = -(\mathrm{I})/\tau_0 \quad (7)$$

and are explicitly given for a system as described in Scheme 2 by

$$\gamma_1 = -k_{03} \quad (8)$$

$$\gamma_{2,3} = -\frac{1}{2}(S_1 + S_2 \pm [\{S_1 - S_2\}^2 + 4P[\mathrm{M}]]^{1/2}) \quad (9)$$

$$S_1 = k_{01} + (k_{21} + k_{31})[\mathrm{M}] \quad (10)$$

$$S_2 = k_{02} + k_{12} + k_{32} \quad (11)$$

$$P = k_{12}k_{21} \quad (12)$$

3.2. Identifiability. The identifiability study examines if the rate constants k_{ij} theoretically can be uniquely determined. Consider the specific case depicted by Scheme 2 with the system matrix **A** given by eq 6. The identifiability study is identical to that derived for PROBE.[23] Therefore, only the results which are relevant for POLYPROBE will be presented here. The same symbols as for the identifiability of the PROBE system[23] will used.

From the exponential factors γ_i at a minimum of two different concentrations the concentration-independent γ (eq 8) can be assigned to k_{03}. At [M] = 0, the decay is monoexponential and yields the unique value for k_{01}. If in addition k_{02} is known, the remaining rate constants, i.e., k_{21}, k_{31}, k_{12}, and k_{32}, can be determined within certain limits by use of the scanning technique.[28] In this technique one of these rate constants is held constant at a preset value while the others are freely adjustable. Defining the parameters A, B^*, and C^* from eqs 13–15

$$A = k_{21} + k_{31} \quad (13)$$

$$B^* = k_{12} + k_{32} \quad (14)$$

$$C^* = k_{12}k_{21} \quad (15)$$

and performing the scanning procedure over a broad range of rate constant values allow one to specify limits on the rate constants k_{21}, k_{31}, k_{12}, and k_{32}:

$$0 < k_{31} < A - C^*/B^* \quad (16)$$

$$C^*/B^* < k_{21} < A \quad (17)$$

$$0 < k_{32} < B^* - C^*/A \quad (18)$$

$$C^*/A < k_{12} < B^* \quad (19)$$

3.3. Data Analysis. It is well known that the global analysis method,[29-31] i.e., when data from several different experiments are analyzed simultaneously with common model parameters partly or totally linked, is generally superior to local (or single-curve) analysis.

The global compartmental analysis program, based on Marquardt's algorithm,[32] has been described elsewhere.[24]

Consider the excited-state processes depicted by Scheme 2. The global fitting parameters are k_{ij}, $\tilde{b}_k$, and $\tilde{c}_k$ and the only local fitting parameters are the scaling factors. Using this approach, experiments done at different excitation/emission wavelengths, at multiple timing calibrations, and at different POLYPROBE and POLYSALT concentrations are linked by all rate con-

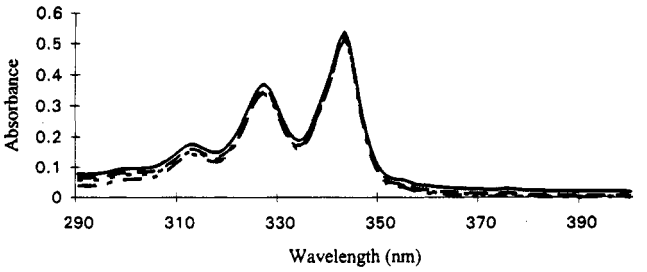

Figure 2. Absorption spectra of POLYPROBE with added POLYSALT: 0 (—), 1×10^{-3} (- - -), 2×10^{-3} (• • •), and 3×10^{-3} M (- • -).

stants defining the system. The fitting parameters were estimated by minimizing the global reduced χ_g^2:

$$\chi_g^2 = \sum_l^q \sum_i w_{li}(y_{li}^o - y_{li}^c)^2/\nu \qquad (20)$$

where the index l sums over q experiments and the index i sums over the appropriate channels for each individual experiment. y_{li}^o and y_{li}^e denote the observed (experimentally measured) and calculated (fitted) values corresponding to the ith channel of the lth experiment, respectively, and w_{li} is the corresponding statistical weight. ν represents the number od degrees of freedom for the entire multidimensional fluorescence decay surface.

The statistical criteria to judge the quality of the fit include both graphical and numerical tests. The graphical methods comprised plots of surfaces of the autocorrelation function values *vs* experiment number and of the weighted residuals *vs* channel number *vs* experiment number. The numerical statistical tests incorporated the calculation of χ_g^2 and its corresponding $Z_{\chi_g^2}$:

$$Z_{\chi_g^2} = (1/2\nu)^{1/2}(\chi_g^2 - 1) \qquad (21)$$

The additional statistical criteria to judge the quality of the fit are described elsewhere.[33]

4. Results and Discussion

4.1. Time-Resolved Fluorescence of POLYPROBE at Very Low Concentration. At a very low concentration (1×10^{-6} M) POLYPROBE decays monoexponentially with a lifetime of 237 ± 1 ns, from which $k_{01} = 4.22 \times 10^6$ s^{-1} is calculated. This value is identical to that found for PROBE,[23] indicating that neither the chain nor the counterion exerts an influence on the decay kinetics.

4.2. Properties of POLYPROBE as a Function of Added Quaternary Ammonium Salt POLYSALT. 4.2.1. Stationary Measurements. Solutions of POLYPROBE (1×10^{-6} M) with increasing concentrations of POLYSALT (0, 1×10^{-3}, 2×10^{-3}, and 3×10^{-3} M) were studied by stationary absorption and emission techniques. Figure 2 displays the absorption spectra of these solutions, and Figures 3 and 4 show the fluorescence emission and excitation spectra, respectively. From these figures it is clear that the addition of POLYSALT does not exert an influence noticeable by the applied techniques.

4.2.2. Time-Resolved Fluorescence Measurements. For the time-resolved measurements two timing calibrations were used: 1.488 ns/channel and 163 ps/channel. The data could not be fitted by a monoexponential function: a biexponential decay function was needed to describe the fluorescence. Both decay times

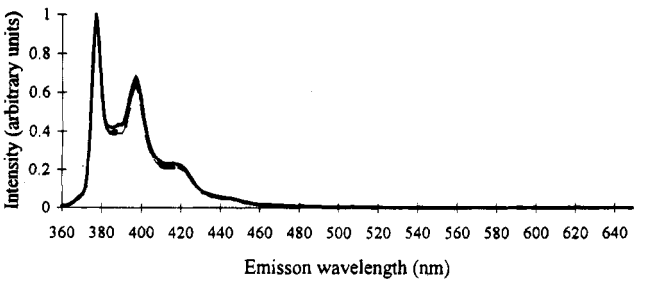

Figure 3. Normalized emission spectra of POLYPROBE with added POLYSALT: 0 (—), 1×10^{-3} (- - -), 2×10^{-3} (• • •), and 3×10^{-3} M (- • -).

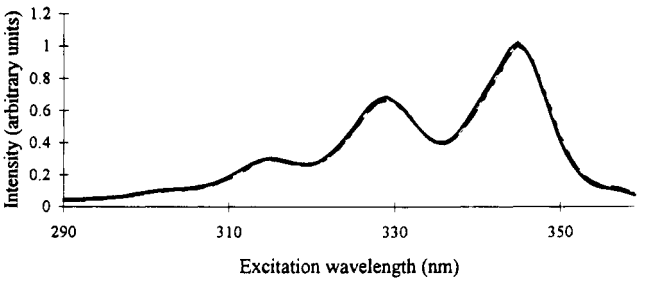

Figure 4. Excitation spectra of POLYPROBE with added POLYSALT: 0 (—), 1×10^{-3} (- - -), 2×10^{-3} (• • •), and 3×10^{-3} M (- • -).

were found to be dependent on the concentration of POLYSALT (Table 1). Since the long decay time increases when going from higher to lower POLYSALT concentrations, we have $k_{02} > k_{01}$.[23,24]

The 24 curves which were globally fitted by a biexponential model were subsequently analyzed in a single step by global bicompartmental analysis (Scheme 3). In this scheme compartment 1 comprises the isolated POLYPROBE, while compartment 2 is the POLYPROBE involved in ion aggregation. Since the fluorescence was recorded at four emission wavelengths and three different salt concentrations, the compartmental system is theoretically identifiable.[26] During the compartmental analysis, the rate constants k_{01}, k_{21}, k_{02}, and k_{12} were globally linked over the whole fluorescence decay surface. The spectral parameters $\tilde{b}_1$ and $\tilde{c}_1$, being functions of the POLYSALT concentration and the emission wavelength, respectively, were regionally linked at the corresponding [POLYSALT] and λ^{em}. The recovered k_{01} corresponds very well to the value obtained at a very low POLYPROBE concentration in the absence of added POLYSALT (section 4.1) and $k_{02} > k_{01}$, as suggested from the decay time analysis. Table 2 compiles the values for the rate constants and the spectral parameters obtained from this analysis. It must be noted that the result $k_{02} > k_{01}$ differs from the results in the analysis of PROBE. For PROBE it was reported[23] that $k_{01} = k_{02}$ and, consequently, it was concluded that the ion aggregation had no influence on the photophysics of the charged probe. The difference between the rate constants in the present system indicates a change in the local environment upon aggregation. The presence of a polymer chain in POLYPROBE and/or the difference in counterion between PROBE (perchlorate) and POLYPROBE (trifluoromethanesulfonate) might be possible causes. To obtain additional proof that the two rate constants were indeed different, the experimental data were fitted by a compartmental model where both rate constants were described by the same parameter. This resulted in unacceptable fits.

If one defines $K^* = k_{21}/k_{12}$, the value obtained is 108 ± 33 M^{-1}. The constant K^* describes the dipole–dipole/

Table 1. Decay Parameters of POLYPROBE (2×10^{-6} M) in THF as a Function of POLYSALT Concentration Estimated by Global Biexponential Analysis[a]

(A) [POLYSALT] = 1×10^{-3} M, $Z_{\chi_R^2} = 1.4$

λ^{em} (nm)	t_i (ns/channel)	α_1	τ_1 (ns)	α_2	τ_2 (ns)
380	1.488	-0.04 ± 0.02	5.7 ± 0.2	0.82 ± 0.01	214.5 ± 0.5
390		-0.04 ± 0.02		0.86 ± 0.01	
400		-0.00 ± 0.03		0.75 ± 0.01	
410		0.02 ± 0.01		0.57 ± 0.01	
380	0.163	0.07 ± 0.01		0.29 ± 0.01	
390		0.07 ± 0.01		0.26 ± 0.01	
400		0.08 ± 0.01		0.25 ± 0.01	
410		0.11 ± 0.01		0.23 ± 0.01	

(B) [POLYSALT] = 2×10^{-3} M, $Z_{\chi_R^2} = 3.8$

λ^{em} (nm)	t_i (ns/channel)	α_1	τ_1 (ns)	α_2	τ_2 (ns)
380	1.488	-0.02 ± 0.01	10.2 ± 0.5	0.82 ± 0.01	208.5 ± 0.3
390		0.00 ± 0.01		0.68 ± 0.01	
400		0.04 ± 0.01		0.73 ± 0.01	
410		0.05 ± 0.01		0.56 ± 0.01	
380	0.163	0.03 ± 0.01		0.35 ± 0.01	
390		0.02 ± 0.01		0.22 ± 0.01	
400		0.03 ± 0.01		0.21 ± 0.01	
410		0.04 ± 0.01		0.21 ± 0.01	

(C) [POLYSALT] = 3×10^{-3} M, $Z_{\chi_R^2} = 2.5$

λ^{em} (nm)	t_i (ns/channel)	α_1	τ_1 (ns)	α_2	τ_2 (ns)
380	1.488	0.00 ± 0.02	7.6 ± 0.2	0.82 ± 0.01	204.9 ± 0.5
390		0.02 ± 0.02		0.66 ± 0.01	
400		0.03 ± 0.03		0.75 ± 0.01	
410		0.08 ± 0.01		0.59 ± 0.01	
380	0.163	0.03 ± 0.01		0.23 ± 0.01	
390		0.02 ± 0.01		0.20 ± 0.01	
400		0.03 ± 0.01		0.20 ± 0.01	
410		0.05 ± 0.01		0.21 ± 0.01	

[a] For each time increment (t_i) four emission wavelengths were used. The excitation wavelength was 320 nm.

Scheme 3

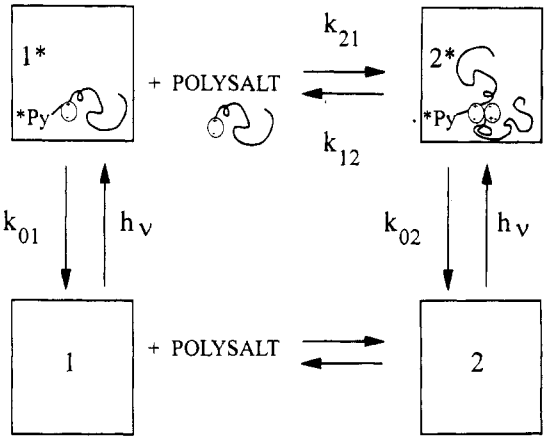

Table 2. Global Bicompartmental Analysis of 24 Decay Curves of POLYPROBE as a Function of Added POLYSALT in THF[a]

Rate Constant Values

$k_{01} = (4.38 \pm 0.05) \times 10^6\ s^{-1}$ $k_{02} = (6.66 \pm 0.07) \times 10^6\ s^{-1}$
$k_{21} = (13 \pm 2) \times 10^9\ M^{-1}\ s^{-1}$ $k_{12} = (12 \pm 1) \times 10^7\ s^{-1}$

[a] For the analysis a $Z_{\chi_R^2}$ of 12.7 was obtained.

ion–dipole association of the quaternary ammonium salt of locally excited POLYPROBE and the quaternary ammonium of POLYSALT. This value can be compared to the value obtained from experiments with PROBE and *N,N,N*-trimethyl-1-dodecanaminium perchlorate as added salt.[23] The reported value for the later system ($700 \pm 130\ M^{-1}$) is about 7 times larger than that for POLYPROBE. Keeping in mind that k_{21} describes the diffusion of two species, this rate constant is thought to be smaller for a molecule attached to a polymer as compared to the polymer-free molecule. Indeed, k_{21} in the present system is about one-third that in the PROBE system, mainly explaining the weaker dipole–dipole/ion–dipole association in the POLYPROBE system.

4.3. Properties of POLYPROBE as a Function of Its Concentration. 4.3.1. Time-Resolved Measurements. The single-photon-timing experiments were performed on solutions differing in POLYPROBE concentration: 2×10^{-3}, 1×10^{-3}, 6×10^{-4}, and 2×10^{-5} M POLYPROBE in THF. Each of these solutions was measured at 30 different emission wavelengths (375–520 nm) and two timing calibrations (1.488 ns/channel and 163 ps/channel). At each POLYPROBE concentration the decays collected as a function of emission wavelength and time increment were globally fitted by a triple-exponential model with linked decay times. This implies a compartmental system with three excited-state species. The stationary emission spectra showed emission from the pyrene excimer (spectra not shown), increasing in relative intensity with increasing POLYPROBE concentration, as was also found for PROBE.[23]

The data acquired in the region where only the monomer emits (375 nm) can be described by a biexponential decay function. A triple-exponential function (eq 5) with two negative preexponential factors and one positive preexponential factor can be fitted to the data recorded in the region where only excimer emission is observed (520 nm). The sum of the three preexponential factors equals zero. For POLYPROBE this means that there are two locally excited states and one excimer excited state. A possible physical model will have to include the ion aggregation of the quaternary ammonium salts in THF. Since the decay traces collected in the region where only the monomer emits (375 nm)

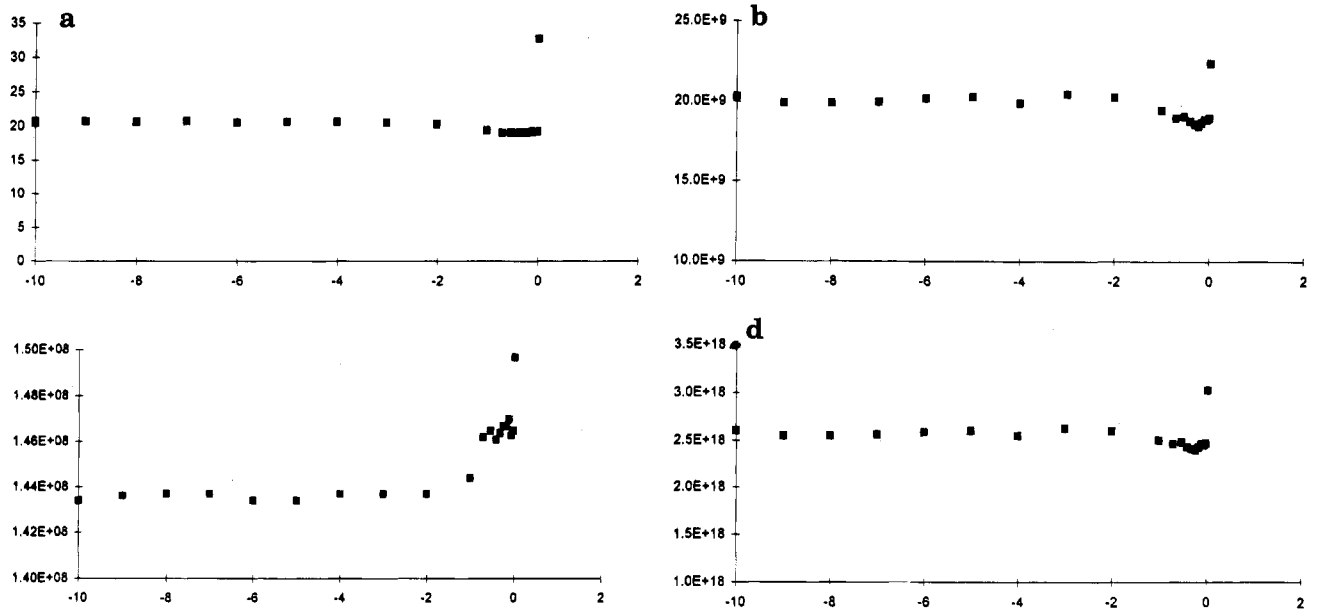

Figure 5. Global compartmental analysis of 60 decay traces of POLYPROBE in THF collected at 30 emission wavelengths between 375 and 500 nm. Two different POLYPROBE concentrations were used: 2×10^{-3} and 1×10^{-3} M at two different timing calibrations (1.488 ns/channel and 163 ps/channel). (A) $Z_{\chi_R^2}$ values (eq 21) as a function of log k_{31}. (B) A values (eq 13) calculated from the scanned k_{31} values and the estimated k_{21} values as a function of log k_{31}. (C) B^* values (eq 14) calculated from the scanned k_{31} and the estimated k_{32} values as a function of log k_{31}. (D) C^* values (eq 15) calculated from the estimated k_{12} and k_{21} values as a function log k_{31}.

Scheme 4

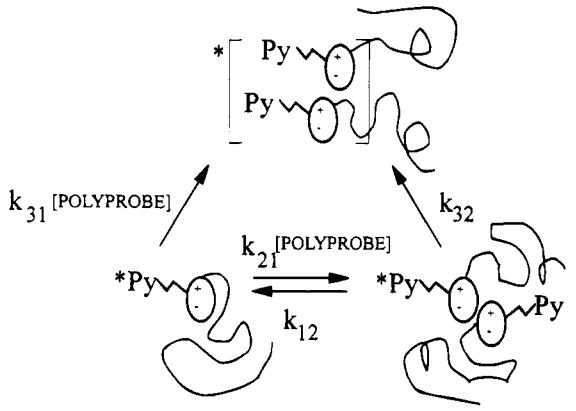

can be described by a biexponential decay function, no excimer dissociation will occur during its lifetime. This means that k_{13} and k_{23} both can be set equal to zero. On the basis of these arguments the model in Scheme 4 can be proposed. The transition from compartment 1 to compartment 2 is an association phenomenon either due to ion–dipole interactions leading to triple ions or due to dipole–dipole interactions.

The identifiability study[23] of the compartmental system depicted in Scheme 4 indicated that k_{01} and k_{03} can be determined in a unique way. Assuming k_{01} and k_{02} to be equal to the values estimated from the concentration study of POLYPROBE and POLYSALT, respectively, and k_{03} to be equal to the value of the concentration-independent γ (eq 8), one can make use the scanning technique to obtain limits on the remaining rate constants[28] (k_{21}, k_{31}, k_{12}, and k_{32}). Hence, the scanning procedure was performed and values for A, B^*, and C^* (eqs 13–15) were estimated from which the bounds on the rate constants can be set (eqs 16–19). In Figure 5 the goodness-of-fit parameter $Z_{\chi_R^2}$ (Figure 5A), A (Figure 5B), B^* (Figure 5C), and C^* (Figure 5D) are shown as a function of the scanned parameter k_{31}. From the estimated values of A (2×10^{10} M^{-1} s^{-1}), B^* (1.45×10^9 s^{-1}), and C^* (2.5×10^{18} M^{-1} s^{-2}), eqs 16–19 give the following limits on the rate constants: $k_{31} < 2.8 \times 10^9$ M^{-1} s^{-1}, $1.7 \times 10^{10} < k_{21} < 2 \times 10^{10}$ M^{-1} s^{-1}, $1.3 \times 10^8 < k_{12} < 1.45 \times 10^8$ s^{-1}, and $k_{32} < 2 \times 10^7$ s^{-1}. Using the maximum and minimum values on k_{21} and k_{12}, we obtain $119 < K^* < 160$ M^{-1}, in very good accordance with the value obtained for the POLYPROBE/POLYSALT system.

Table 3. Estimated Kinetic Parameters of the Charged Fluorescent Probe PROBE[23] and POLYPROBE in THF

	PROBE	POLYPROBE	POLYPROBE + POLYSALT
k_{21} (10^9 M^{-1} s^{-1})	53–60	17.2–20	13
k_{31} (10^9 M^{-1} s^{-1})	<7	<2.8	
k_{12} (10^9 s^{-1})	0.15–0.17	0.125–0.145	0.12
k_{32} (10^9 s^{-1})	<0.02	<0.02	
K^* (M^{-1})	356 ± 44	140 ± 20	108 ± 33

The estimated kinetic parameters of PROBE and POLYPROBE in THF are compiled in Table 3. All values for POLYPROBE were found to be smaller than those of PROBE. It can be readily seen that the rate constants connected to intermolecular diffusion processes (k_{21} and k_{31}) are both smaller for POLYPROBE than the corresponding values from the PROBE system, as would be expected. The rate constants describing the intramolecular rearrangements, however, take similar values in both systems, indicating that the dipole–dipole/ion–dipole rearrangements are not affected by the presence of the polymer chain.

The ranges of the values of k_{21}, k_{12}, and K^* obtained for POLYPROBE are very similar to the corresponding values when POLYSALT is added. This indicates that the same interactions play in these two system.

The decay times τ_i (eqs 8 and 9) as a function of the POLYPROBE concentration ([M]) can be calculated using the estimated values for the rate constants and [M]. For k_{01}, k_{02}, and k_{03} the uniquely determined values can be used. For the other rate constants—which are known within certain limits—an arbitrary value of k_{31} in the region where A, B^*, and C^* are constant can be used together with the corresponding values of k_{21}, k_{12}, and k_{32}. The calculated decay times are shown in

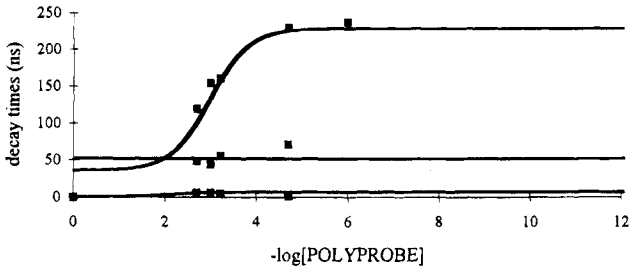

Figure 6. Decay times as a function of −log[M] calculated with the values of the rate constants estimated by global compartmental analysis (see text for details). The decay times estimated by global triple-exponential analysis are shown as the larger squares.

Figure 6. The decay times estimated by global triexponential analysis are also shown in this figure and agree perfectly with those obtained through global compartmental analysis, giving further evidence on the consistency of the analysis and interpretations.

5. Conclusions

This paper describes a systematic way to unravel the association−dissociation kinetics of the halato telechelic polymer POLYPROBE in THF by use of time-resolved fluorescence measurements. The system is described in terms of compartments, and three different compartments could be found: (1) the isolated POLYPROBE molecule, (2) two POLYPROBE molecules involved in ion aggregation, and (3) ion-aggregating POLYPROBE molecules where their pyrene chromophores form an excimer. From measurements on a solution with a very low POLYPROBE concentration, the rate constant for deactivation from compartment 1 can be determined from the monoexponential fluorescence decay. Adding the corresponding halato telechelic polymer without chromophore, POLYSALT, results in a biexponential decay. Bicompartmental analysis gives the value of the rate constant for deactivation from compartment 2. Finally, measuring the fluorescence emission as a function of POLYPROBE concentration results in the remaining deactivation rate from compartment 3. It is also concluded that the interconversions from compartment 3 to any of the others are negligibly slow. For the other rate constants for interconversion between the three compartments, however, no unique values can be estimated. By the use of the scanning technique in global compartmental analysis, upper and lower limits can be calculated for these rate constants. Comparing the results obtained for a similar chromophore, but without a polymer chain attached to it, shows that the rate constants connected to bimolecular diffusion processes take lower values upon attaching a polymer chain to the fluorophore. The rate constants of intramolecular processes, i.e., dissociation of and chromophore rearrangement within an ion-aggregated dimer, however, are not affected by the presence of a polymer chain.

Acknowledgment. B.H. thanks the I.W.O.N.L. for a predoctoral fellowship. J.v.S. thanks the Swedish Natural Science Research Council (NFR) for a postdoctoral grant through the European Human Capital and Mobility Scheme. N.B. is an Onderzoeksleider of the Belgian Fonds voor Geneeskundig Wetenschappelijk Onderzoek (FGWO). Marcel Ameloot is thanked for fruitful discussions. The financial support through IUAP-III-040 and IUAP-II-16 is gratefully acknowledged.

References and Notes

(1) Lundberg, R. D. *Structure and Properties of Ionomers*; Pineri, M., Eisenberg, A., Eds.; NATO ASI Series; D. Reidel: Dordrecht, 1987; p 387.
(2) Hara, M.; Lee. A. H.; Wu, J. *J. Polym. Sci., Part B: Polym. Phys.* **1987**, *25*, 1407.
(3) Lantman, C. W.; MacKnight, W. J.; Peiffer, D. G.; Sinha, S. K.; Lundberg, R. D. *Macromolecules* **1987**, *20*, 1096.
(4) Hara, M.; Wu, J.; Lee, A. *Macromolecules* **1988**, *21*, 2214.
(5) Hara, M.; Wu, J.; Lee, A. *Macromolecules* **1989**, *22*, 754.
(6) Kocak, H. I.; Aras, L. *Polymer* **1990**, *31*, 1328.
(7) Bockris, J.; Reddy, A. *Modern Electrochemistry*; Plenum Press: New York, 1970.
(8) Hara, M.; Wu, J. *Macromolecules* **1988**, *21*, 402.
(9) Pedley, A. M.; Higgins, J. S.; Peiffer, D. G.; Burchard, W. *Macromolecules* **1990**, *23*, 1434.
(10) Lantman, C. W.; MacKnight, W. J.; Higgins, J. S.; Peiffer, D. G.; Sinha, S. K.; Lundberg, R. D. *Macromolecules* **1988**, *21*, 1339.
(11) Gabrys, B.; Higgins, J. S.; Lantman, C. W.; MacKnight, W. J.; Pedley, A. M.; Peiffer, D. G.; Rennie, A. R. *Macromolecules* **1989**, *22*, 3746.
(12) Pedley, A. M.; Higgins, J. S.; Peiffer, D. G.; Rennie, A. R. *Macromolecules* **1989**, *22*, 3746.
(13) Feng, D.; Wilkes, G. L. *Macromolecules* **1991**, *24*, 3746.
(14) Dowling, K. C.; Thomas, J. K. *Macromolecules* **1991**, *24*, 4123.
(15) Bakeev, K. N.; MacKnight, W. J. *Macromolecules* **1991**, *24*, 4578.
(16) Broze, G.; Jérôme, R.; Teyssié, Ph. *Macromolecules* **1982**, *15*, 920.
(17) Broze, G.; Jérôme, R.; Teyssié, Ph. *Macromolecules* **1982**, *15*, 1300.
(18) Broze, G.; Jérôme, R.; Teyssié, Ph.; Marco, C. *Macromolecules* **1983**, *16*, 996.
(19) Jérôme, R.; Broze, G.; Teyssié, Ph. *Microdomains in Polymer Solutions*; Dubin, P., Ed.; Plenum: New York, 1985 (*Polym. Sci. Technol.* **1985**, *30*, 243).
(20) Jérôme, R. *Structure and Properties of Ionomers*; Pineri, M., Eisenberg, A., Eds.; NATO ASI Series; D. Reidel: Dordrecht, 1987, p 399.
(21) Jérôme, R.; Henrioulle-Granville, M.; Boutevin, B.; Robin, J. J. *Prog. Polym. Sci.* **1991**, *16*, 837.
(22) Granville, M.; Jérôme, R.; Teyssié, Ph.; De Schryver, F. C. *Macromolecules* **1988**, *21*, 2894.
(23) Hermans, B.; De Schryver, F. C.; Boens, N.; Ameloot, M.; Jérôme, R.; Teyssié, Ph.; Goethals, E.; Schacht, E. *J. Phys. Chem.* **1994**, *98*, 13583.
(24) Boens, N.; Janssens, L.; De Schryver, F. C. *Biophys. Chem.* **1989**, *33*, 77.
(25) (a) Demas, J. N.; Crosby, G. A. *J. Phys. Chem.* **1971**, *75*, 991. (b) Morris, J. V.; Mahaney, M. A.; Huber, J. R. *J. Phys. Chem.* **1976**, *80*, 969.
(26) Ameloot, M.; Boens, N.; Andriessen, R.; Van den Bergh, V.; De Schryver, F. C. *J. Phys. Chem.* **1991**, *95*, 2041.
(27) Andriessen, R.; Boens, N.; Ameloot, M.; De Schryver, F. C. *J. Phys. Chem.* **1991**, *95*, 2047.
(28) Van Dommelen, L.; Boens, N.; Ameloot, M.; De Schryver, F. C.; Kowalczyk, A. *J. Phys. Chem.* **1993**, *97*, 11738.
(29) (a) Knutson, J. R.; Beechem, J. M.; Brand, L. *Chem. Phys. Lett.* **1983**, *102*, 501. (b) Beechem, J. M.; Knutson, J. R.; Brand, L. *Photochem. Photobiol.* **1983**, *37*, Abstr. S20. (c) Beechem J. M.; Ameloot, M.; Brand, L. *Anal. Instrum.* **1985**, *14*, 379. (d) Beechem, J.; Ameloot, M.; Brand, L. *Chem. Phys. Lett.* **1985**, *120*, 466.
(30) (a) Löfroth, J.-E. *Anal. Chem.* **1985**, *14*, 403. (b) Löfroth, J.-E. *Eur. Biophys. J.* **1985**, *13*, 45.
(31) Janssens, L. D.; Boens, N.; Ameloot, M.; De Schryver, F. C. *J. Phys. Chem.* **1990**, *94*, 3564.
(32) Marquardt, D. W. *J. Soc. Ind. Appl. Math.* **1963**, *11*, 431.
(33) Boens, N. In *Luminescence Techniques in Chemical and Biochemical Analysis*; Baeyens, W. R. G., De Keukeleire, D., Korkidis, K., Eds.; Marcel Dekker: New York, 1991; p 21.
(34) Van den Bergh, V.; Kowalczyk, A.; Boens, N.; De Schryver, F. C. *J. Phys. Chem.* **1994**, *98*, 9503.

MA946113I